arXiv:1006.3282v4 [quant-ph] 26 Sep 2011

Analysis of quantum coherence in bismuth-doped silicon: a system of strongly coupled spin qubits

M. H. Mohammady,[1] G. W. Morley,[1,2] A. Nazir,[1,3] and T. S. Monteiro[1]
[1]*Department of Physics and Astronomy, University College London,*
Gower Street, London WC1E 6BT, United Kingdom
[2]*London Centre for Nanotechnology University College London,*
Gordon Street, London WC1H 0AH, United Kingdom
[3]*Blackett Laboratory, Imperial College London, London SW7 2AZ, United Kingdom*

(Dated: September 27, 2011)

We investigate bismuth-doped silicon (Si:Bi) in the "nuclear-electronic" regime where the hyperfine coupling of 1.4754 GHz is comparable to the electron Zeeman term in the spin Hamiltonian. This corresponds to intermediate magnetic fields, $B \approx 0.1 - 0.6$ T. There is growing interest in Si:Bi as an alternative to the well-studied proposals for silicon based quantum information processing (QIP) using phosphorus-doped silicon (Si:P). We focus here on the implications of the anomalously-strong hyperfine coupling. In particular, we analyse in detail the regime where recent 4 GHz pulsed magnetic resonance experiments have demonstrated orders of magnitude speed-up in quantum gates involving transitions which are forbidden at high fields. We also present calculations using a phenomenological Markovian master equation which models the decoherence of the electron spin due to Gaussian temporal magnetic field perturbations. The model quantifies the advantages of certain "optimal working points" identified as the $\frac{df}{dB} = 0$ regions, which come in the form of frequency minima and maxima. We show that at such regions, dephasing due to the interaction of the electron spin with a fluctuating magnetic field in the z direction (usually adiabatic) is completely removed.

PACS numbers: 03.67.Lx,03.67.-a,76.30-v,76.90.+d,

I. INTRODUCTION

Beginning with the seminal proposal by Kane [1], there has been intense interest, for over a decade, in the use of Si:P [2] as qubits for quantum information processing. This donor-impurity spin-system continues to demonstrate an ever-increasing list of advantages for manipulation and storage of quantum information with currently available electron paramagnetic resonance (EPR) and nuclear magnetic resonance (NMR) technology. The Si:P system has four levels due to the electron spin $S = \frac{1}{2}$ coupled to a ^{31}P nuclear spin $I = \frac{1}{2}$.

The key advantages are the comparatively long decoherence times, which have been measured to be of order milliseconds for the electron spin, for natural Si:P. They are of order seconds for the nuclear spin, so the nuclear spin has been identified [1] as a resource for storing the quantum information. For all but the weakest magnetic fields (i.e. $B_0 \gtrsim 200$G) [3], the electron and nuclear spins are uncoupled so may be addressed and manipulated independently by a combination of microwave (mw) and radio-frequency (rf) pulses respectively. The two possible electron-spin transitions correspond to EPR spectral lines, while the nuclear spin transitions are NMR lines. Nuclear spin-flips are much slower: a π-pulse in the NMR case takes three orders of magnitude longer than for the EPR-allowed transitions.

However, over the last year or so, there has also been increasing interest in another shallow donor impurity in silicon, the bismuth atom [4–8]. The Si:Bi system is unique in several respects: it is the deepest donor, with a binding energy of about 71 meV; it has a very large nuclear spin, $I = 9/2$; it has an exceptionally large hyperfine coupling strength, $\frac{A}{2\pi} = 1.4754$ GHz; in addition, ^{209}Bi is monoisotopic. Recent measurements of the decoherence times in natural silicon have revealed T_2 times of order 30% larger than for Si:P, an effect attributed to the smaller Bohr radius of Si:Bi [5]. The dominant decoherence process is the spin diffusion [9, 10] associated with the $I = 1/2$, ^{29}Si nuclei occupying just under 5% of sites in natural silicon; the dominant ^{28}Si isotope has no nuclear spin and thus does not contribute to the dipole-coupled flip-flop process which drives the spin diffusion. A recent study of P donors in ^{28}Si purified to such a high degree (less than 50 ppm of ^{29}Si) that spin diffusion may be neglected, revealed T_2 times potentially up to 10s [11]. Although studies of isotopically enriched Si:Bi have yet to be undertaken, decoherence times of the same order are possible. The coupling with ^{29}Si was investigated in [8]. The very large nuclear spin $I = 9/2$ and associated large Hilbert space may provide a means of storing more information [4]. Efficient hyperpolarization of the system (to about 90%) was demonstrated experimentally in [6].

The present study investigates the implications of the very large hyperfine coupling, $\frac{A}{2\pi} = 1.4754$ GHz of Si:Bi, as well as its large nuclear spin. While mixing of the Zeeman sublevels $|m_S, m_I\rangle$ is not unexpected and has even been investigated for Si:P for weak magnetic fields [3], for Si:Bi the regime where the hyperfine coupling competes with the external field, i.e. $A \sim \mu B_0/\hbar$, is attained for magnetic fields $B_0 \simeq 0.1 - 0.6$ T which are moderate, but within the normal EPR range. In a previous paper [7] we identified interesting consequences in this range of magnetic fields. In particular, we identified a set of points and field values associated with "cancellation resonances", thus named because of an analogy with the electron spin echo envelope modulation (ESEEM) phenomenon of "exact cancellation" [12]. At the cancellation resonances, as we see below, the system Hamiltonian takes a simpler form. Here we investigate the relative advantages of these regimes for QIP.

A recent experimental study using an S-band (4 GHz) pulsed EPR spectrometer [13] identified a set of 4-states of Si:Bi which are, at high fields, entirely analogous to the 4-level subspace of Si:P but have the advantage that all four possible transitions may be driven by fast EPR transitions (on a nanosecond timescale), in contrast to Si:P, where the two NMR transitions are three orders of magnitude slower. The study showed that for Si:Bi in the intermediate field regime, it is possible to equalize the time for a π-rotation of two transitions which correspond to an EPR and NMR transition respectively, at high fields. We show that this represents a novel scheme to implement universal quantum computation using, exclusively, fast EPR technology. This represents a clear advantage offered by the Si:Bi system.

In [7], it was suggested that the "cancellation resonance" points might offer further advantages in minimising and controlling exchange coupled perturbations. Here we do not investigate this, but consider effects of Z-noise and X-noise (in other words Gaussian temporal magnetic-field fluctuations along the X and Z direction) on decoherence. This may be relevant to the behavior of isotopically enriched Si:Bi. We show that for Z noise, which is usually adiabatic, the $\frac{df}{dB} = 0$ points offer decoherence-free zones. In analogy with work done on superconducting qubits [14], we call these "optimal working points". The system does not show such advantages for X noise, however, which leads to temperature-independent depolarising noise.

In section II we introduce the Hamiltonian for coupled nuclear-electronic spin systems for $S = 1/2$ and arbitrary I. We explain the analogy between the EPR hyperfine cancellation resonances and the Electron Spin Echo Envelope Modulation (ESEEM) regime of exact cancellation. We also introduce the individual resonances, describe salient features and present time-dependent calculations. In Section III we introduce the system as a pair of coupled qubits and compare with Si:P. We propose here a scheme of universal two-qubit quantum computation. In section IV we introduce a model of decoherence caused by a temporal fluctuation of the external magnetic field, and study the effect of the cancellation resonances on the decoherence rates this model predicts. We conclude in Section V.

II. THEORY OF COUPLED NUCLEAR-ELECTRONIC SPIN SPECTRA

A. The Hamiltonian

nuclear-electronic spin systems such as Si:P and Si:Bi are described by the Hamiltonian:

$$\hat{H}_0 = \omega_0 \hat{S}_z - \omega_0 \delta \hat{I}_z + A \hat{\mathbf{S}}.\hat{\mathbf{I}} \tag{1}$$

where ω_0 represents the electron Zeeman frequency given by $Bg\beta$. Here B is the strength of the external magnetic field along the z direction, g is the electron g-factor, and β is the Bohr magneton. $\delta = \omega_I/\omega_0 = 2.488 \times 10^{-4}$ represents the ratio of the nuclear to electronic Zeeman frequencies. A is the isotropic hyperfine interaction strength. The operators $\hat{\mathbf{S}}$ and $\hat{\mathbf{I}}$ act on the electronic and nuclear spins, respectively. The total spin of the electron and nucleus is given by S and I, and their z-axis projection by m_S and m_I, respectively.

For the systems considered, the electron spin is always $S = \frac{1}{2}$. As a result the dimension of the Hilbert space is determined by the particular nuclear spin: for a given nuclear spin I, there are $2(2I+1)$ eigenstates which can be superpositions of spin basis states $|m_s, m_I\rangle$. However, since $[\hat{H}_0, \hat{S}_z + \hat{I}_z] = 0$, the Hamiltonian in Eq.(1) decouples to a direct sum of one and two-dimensional sub-Hamiltonians H_m^{1d} and H_m^{2d} with constant $m = m_s + m_I$. The former act on the basis states $|m_S = \pm\frac{1}{2}, m_I = \pm(I + \frac{1}{2})\rangle$, while the latter act on the basis states $|m_S = \pm\frac{1}{2}, m_I = m \mp \frac{1}{2}\rangle$ such that $|m| < I + \frac{1}{2}$. The two-dimensional sub-Hamiltonians can be expanded in the Pauli basis. In particular, the external field part of the sub-Hamiltonian operator is given in matrix form:

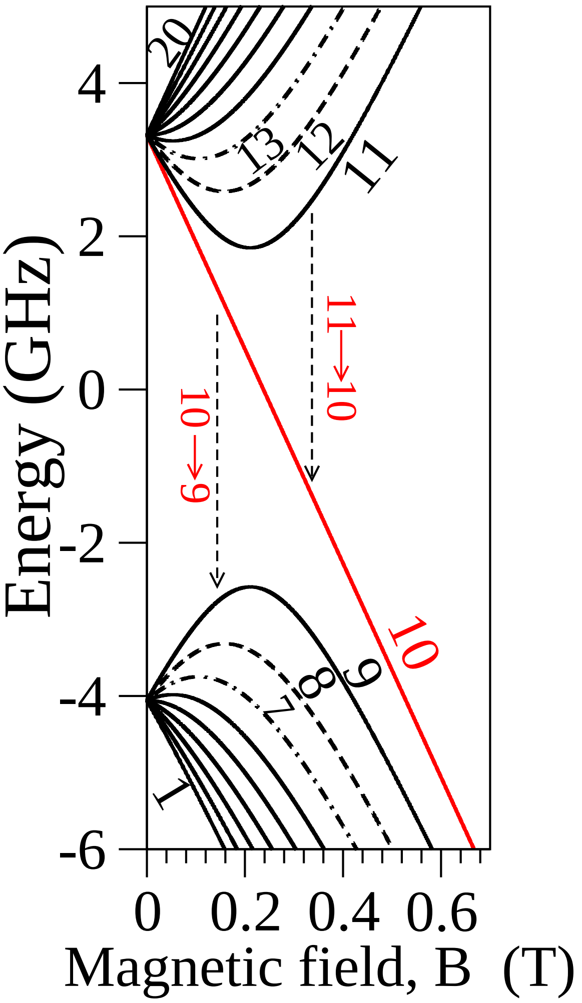

FIG. 1: The 20 spin energy-levels of Si:Bi may be labelled in order of increasing energy $|1\rangle, |2\rangle ... |20\rangle$. States $|10\rangle$ and $|20\rangle$ are not mixed. State $|10\rangle$ is of especial significance since it, rather than the ground state, is a favourable state to initialise the system in. Experimental hyperpolarization studies [6] concentrate the system in this state. Thus, in our coupled 2-qubit scheme, state $|10\rangle$ corresponds to our $|0_e 0_n\rangle$ state; in the same scheme, states $|9\rangle \equiv |0_e 1_n\rangle$ and $|11\rangle \equiv |1_e 0_n\rangle$ are related to $|10\rangle$ by a single qubit flip while for $|12\rangle \equiv |1_e 1_n\rangle$ both qubits are flipped.

$$\omega_0 \hat{S}_z - \omega_0 \delta \hat{I}_z = \frac{\omega_0}{2} \left[(1+\delta)\sigma_z - 2m\delta \mathbb{1} \right]. \tag{2}$$

The z-component of the hyperfine coupling:

$$A \hat{S}_z \otimes \hat{I}_z = \frac{A}{2} \left(m\sigma_z - \mathbb{1}/2 \right) \tag{3}$$

is seen to have an isotropic component as well as a non-isotropic component dependent on σ_z, while the x, y components are given by:

$$A(\hat{S}_x \otimes \hat{I}_x + \hat{S}_y \otimes \hat{I}_y) = \frac{A}{2}(I(I+1) + \frac{1}{4} - m^2)^{1/2}\sigma_x. \quad (4)$$

Summing the above terms gives each H_m^{2d}, whereas only Eqs. (2) and (3) contribute to H_m^{1d}:

$$\begin{aligned} H_m^{2d} &= \frac{A}{2}\left(\Delta_m \sigma_z + \Omega_m \sigma_x - \epsilon_m \mathbb{1}\right) \\ H^{1d}_{m=\pm(I+\frac{1}{2})} &= \frac{A}{2}(\pm\Delta_m - \epsilon_m) \\ \Delta_m &= m + \tilde{\omega}_0(1+\delta) \\ \Omega_m &= (I(I+1) + \frac{1}{4} - m^2)^{1/2} \\ \epsilon_m &= \frac{1}{2}(1 + 4\tilde{\omega}_0 m\delta). \end{aligned} \quad (5)$$

$\tilde{\omega}_0 = \frac{\omega_0}{A}$ is the rescaled Zeeman frequency. We define a parameter $R_m^2 = \Delta_m^2 + \Omega_m^2$ where R_m represents the vector sum magnitude of spin x and z components in the Hamiltonian. We denote θ_m as the inclination of R_m to the z-axis, such that $\cos\theta_m = \Delta_m / R_m$ and $\sin\theta_m = \Omega_m / R_m$. Then, H_m^{2d} can also be written:

$$H_m^{2d} = \frac{A}{2}\left(R_m \cos\theta_m \sigma_z + R_m \sin\theta_m \sigma_x - \epsilon_m \mathbb{1}\right) \quad (6)$$

The range of values that θ_m can take are given by:

$$\theta_m \in \begin{cases} [0, \arctan\left(\frac{\Omega_m}{|m|}\right)] & \text{such that } m > 0 \\ [0, \frac{\pi}{2}] & \text{such that } m = 0 \\ [0, \frac{\pi}{2} + \arctan\left(\frac{\Omega_m}{|m|}\right)] & \text{such that } m < 0 \end{cases} \quad (7)$$

where the minimal value occurs as $B \to \infty$ and the maximal value occurs at $B = 0$. Note that $\theta_m < \pi \ \forall \ B$.

Straightforward diagonalisation of H_m^{2d} then gives the eigenstates at arbitrary magnetic fields:

$$|\pm, m\rangle = a_m^{\pm}|\pm\frac{1}{2}, m \mp \frac{1}{2}\rangle + b_m^{\pm}|\mp\frac{1}{2}, m \pm \frac{1}{2}\rangle \quad (8)$$

where

$$a_m^{\pm} = \cos\left(\frac{\theta_m}{2}\right) \quad , \quad b_m^{\pm} = \pm\sin\left(\frac{\theta_m}{2}\right) \quad (9)$$

and with the corresponding eigenenergies:

$$E_m^{\pm} = \frac{A}{2}\left[-\frac{1}{2}(1 + 4\tilde{\omega}_0 m\delta) \pm R_m\right]. \quad (10)$$

For H_m^{2d}, $\theta_m = \pi/2$ whenever $m + \tilde{\omega}_0(1+\delta) = 0$, which occurs only for $-I + \frac{1}{2} \leq m \leq 0$. The $B \to \infty$ limit corresponds to $\theta_m \to 0$, such that the eigenstates in Eq.(8) tend to the $|m_S, m_I\rangle$ basis states, which we call the high-field limit states. The higher the hyperfine constant A, the higher the magnetic field would have to be for these eigenstates to be approximated by the high-field limit states. H_m^{1d} has $\theta_m = 0 \ \forall \ m$, and hence gives the uncoupled eigenstates $|\pm\frac{1}{2}, \pm(I + \frac{1}{2})\rangle$ at all magnetic fields. These have the simplified eigenenergies:

$$E_{m=\pm(I+1/2)} = \pm\frac{\omega_0}{2}(1 - 2\delta I) + \frac{AI}{2}. \quad (11)$$

It is important to stress that the σ_z, σ_x above are quite unrelated to the $\hat{S}_z, \hat{S}_x$ electronic spin operators. They are simply a method of representing the two-dimensional sub-Hamiltonians. It also makes obvious that the magnetic fields for which $m + \tilde{\omega}_0(1+\delta) = 0$ are special: here the term in H_m^{2d} dependent on σ_z vanishes entirely. These correspond to Landau-Zener crossings. The point at which $m + \tilde{\omega}_0(1+\delta) = 0$ for $m = -(I + \frac{1}{2})$ also has special properties, although different than those of the previous case. In [7] a further point specific for Si:Bi, for which $\omega_0 = 7A$, was also identified; here $H_m^{2d} \propto (\sigma_x + \sigma_z)$ (ignoring the trivial term proportional to the identity). These field values were all classed as "cancellation resonances" and all have potential applications in QIP.

In Fig.1 the exact expressions in Eqs.(10),(11) were used to reproduce the spin spectra investigated for Si:Bi in e.g. [4] and [6]. These equations can be used to describe any arbitrary coupled nuclear-electronic spin system obeying the Hamiltonian Eq.(1), such as other donor systems in Si including P and As. However, throughout this paper we only use Si:Bi as the instantiated system for which we give numerical solutions.

B. EPR transitions

The EPR transitions $|+, m\rangle \leftrightarrow |-, m-1\rangle$ are dipole allowed at all fields. Their relative intensities are $I \propto 2I^{+\to-}_{m\to m-1}|\langle m_s = \frac{1}{2}|S_x|m_s' = \frac{1}{2}\rangle|^2$. Since $|\langle\frac{1}{2}|S_x| - \frac{1}{2}\rangle|^2 = 1/2$, variations in line intensities arise from the mixing of the states.

$$I^{+\to-}_{m\to m-1} \propto |a_m^+|^2|a_{m-1}^-|^2 = \frac{1}{4}(1 + \cos\theta_m)(1 + \cos\theta_{m-1}) \quad (12)$$

If mixing is significant $|+, m\rangle \leftrightarrow |+, m-1\rangle$ transitions (of intensity I_m^+) and $|-, m-1\rangle \leftrightarrow |-, m\rangle$ transitions (of intensity I_m^-), which are EPR-forbidden (but NMR-allowed) at high field, become strong, with relative intensities:

$$I^+_{m\to m-1} \propto |a_m^+|^2|b_{m-1}^+|^2 = \frac{1}{4}(1 + \cos\theta_m)(1 - \cos\theta_{m-1}) \quad (13)$$

and

$$I^-_{m-1\to m} \propto |a_{m-1}^-|^2|b_m^-|^2 = \frac{1}{4}(1 - \cos\theta_m)(1 + \cos\theta_{m-1}). \quad (14)$$

EPR-forbidden lines disappear at high fields; as $\omega_0 \to \infty$, one can see from Eq.(8) that $I_{\pm, m\leftrightarrow m-1} \sim \frac{1}{\omega_0^2} \to 0$ since $|b_m^-|^2 \propto \frac{1}{\omega_0^2}$ at high fields. Eqs.(10),(12), (13) and (14) are exact so are in complete agreement with numerical diagonalisation of the full Hamiltonian.

C. The $\tilde{\omega}_0 = 1, 2, 3, 4$ cancellation resonances and the frequency minima

These cancellation resonances are Landau-Zener or avoided crossings, when the σ_z term of H_m^{2d} vanishes, leading to "Bell-like" eigenstates in the spin basis. In Fig.2 we

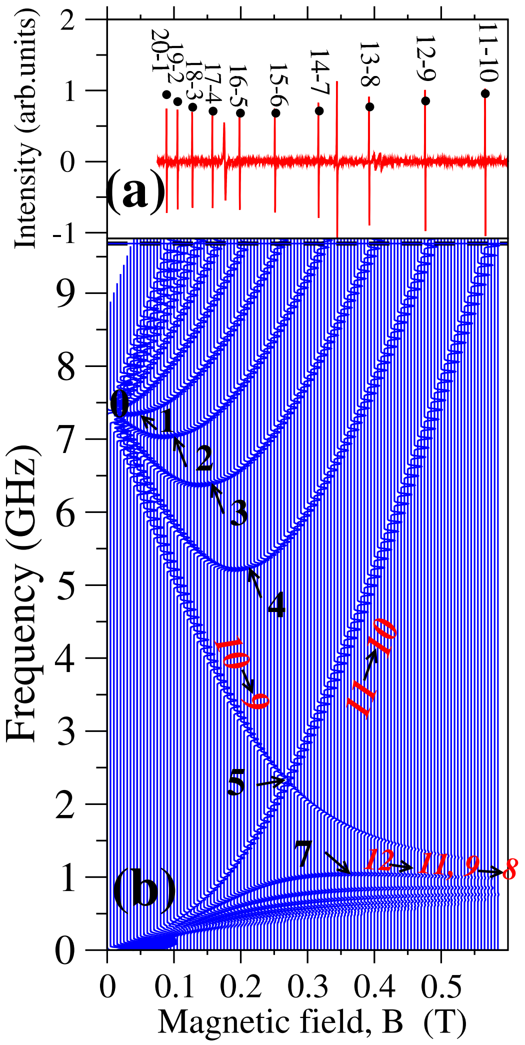

FIG. 2: **(a)** Comparison between theory(Eqs.(10), (11) and (12)) (black dots) and experimental CW EPR signal (red online) at 9.7 GHz. Resonances without black dots above them are not due to Si:Bi; The large sharp resonance at 0.35 T is due to silicon dangling bonds while the remainder are due to defects in the sapphire ring used as a dielectric microwave resonator. The variation in relative intensities is mainly due to the mixing of states as in Eq.(8). The variability is not too high but the calculated intensities are consistent with experiment and there is excellent agreement for the line positions. **(b)** Calculated EPR spectra (convolved with a 0.42 mT measured linewidth); they are seen to line-up with the experimental spectra at $f = \frac{\omega}{2\pi} = 9.7$ GHz). The "cancellation resonances" are indicated by arrows and integers $-m = 0, 1, 2, 3, 4 \ldots$. The $\omega_0 = 7A$ maximum of $\frac{df}{dB}$ indicated by the integer 7 corresponds to that shown in the $\lesssim 2$ GHz Electron Nuclear Double Resonance (ENDOR) spectra of [5].

see several transitions of type $|+, m\rangle \leftrightarrow |-, m-1\rangle$ that have a minimum frequency, closely related to the cancellation resonances. We can show that these minima (obtained by setting $\frac{\partial(R_m + R_{m-1})}{\partial B} = 0$) occur for:

$$\cos\theta_m = -\cos\theta_{m-1} \tag{15}$$

if $m \leq 0$. This implies:

$$\begin{aligned}\theta_m &= \frac{\pi}{2} - \phi \\ \theta_{m-1} &= \frac{\pi}{2} + \phi \end{aligned} \tag{16}$$

which means that the minima lie exactly midway *in angular coordinates* between cancellation resonances. For example, for the $|12\rangle \leftrightarrow |9\rangle$ line ($|+, m=-3\rangle \leftrightarrow |-, m=-4\rangle$) the minimum is at $\omega_0 = \frac{25A}{7} = 3.57A$ so $B = 0.188$ T. Here, R_{-4} has passed its resonance point at 0.21 T (for which $\theta_{-4} = \pi/2$) by an angle $\phi = \arccos\frac{21}{15\sqrt{2}}$ and R_{-3} is at an equal angular distance *before* its resonance at $\simeq 0.16$ T. It has already been shown that a reduction in df/dB results in experimentally measured reductions in decoherence time [5]. The $df/dB = 0$ points imply a reduction in the sensitivity to temporal magnetic fluctuations. In section IV we study how these frequency minima affect decoherence rates caused by Gaussian temporal magnetic-field fluctuations.

D. The $\tilde{\omega}_0 = 7$ resonance; a frequency maximum

The cluster of lines in Fig.2(b) at frequencies $f \lesssim 1$ GHz represent $|\pm, m\rangle \rightarrow |\pm, m-1\rangle$ transitions EPR-forbidden at high B (their intensity is seen to tend to zero for $B \gtrsim 0.5$ T). These transition frequencies have maximal values calculated by setting $\frac{\partial(R_m - R_{m-1})}{\partial B} = 0$, which leads to :

$$\cos\theta_m = \cos\theta_{m-1} \tag{17}$$

if $m \leq 0$. Since $0 \leq \theta_m < \pi$, this implies that $\theta_m = \theta_{m-1}$. Only one such maxima, for the transition $|\pm, -3\rangle \leftrightarrow |\pm, -4\rangle$ occurring at $\tilde{\omega}_0 = 7$ and $B \simeq 0.37$ T can be observed by EPR, however. The other maxima occur at fields $B > 0.5$ T for which the EPR line intensities become vanishingly small. The $\tilde{\omega}_0 = 7$ frequency minima is also classified as a cancelation resonance because of the symmetric property that the H_m^{2d} involved exhibit. This resonance occurs when $\theta_{-3} = \theta_{-4} = \pi/4$, which implies that $H_{-3}^{2d} \propto H_{-4}^{2d} \propto (\sigma_x + \sigma_z)$.

The $\tilde{\omega}_0 = 7$ cancellation resonance offers possibilities for more complex manipulations. It has been suggested [4, 5] that the larger state-space of Si:Bi may be used to store more information. Thus we can show that at $\omega_0 \simeq 7A$, a single EPR (~ 80 ns) pulse can map any coherences between the $m = -4$ states into the same coherences between the $m = -3$ states. The condition Eq.(17) implies that the amplitudes $a_{-3}^{\pm} = a_{-4}^{\pm}$ and $b_{-3}^{\pm} = \pm b_{-4}^{\pm}$. This means that an EPR pulse will effect the rotations $|12\rangle \leftrightarrow |11\rangle$ and $|9\rangle \leftrightarrow |8\rangle$ at the same rate. For instance, if the initial two-qubit state is $|\Psi\rangle = c_{11}|12\rangle + c_9|8\rangle$ a π-pulse will yield $|\Psi\rangle = c_{11}|11\rangle - c_9|9\rangle$, and so produces a mechanism for temporarily storing the two-qubit state (within a relative π phase shift). This is illustrated in Fig.3.

E. The $\tilde{\omega}_0 = 5$ resonance : two-photon transitions

The $m = -5$ state, $|10\rangle$, is not associated with an anti-crossing at any field as the Hamiltonian leaves it uncoupled to any other basis state. Nevertheless the fields for which $m + \tilde{\omega}_0 \approx 0$ (at $\omega_0 \approx 0.26$ T) represent the most drastic type of cancellation: the Δ_{-5} term in H_{-5}^{1d} vanishes,

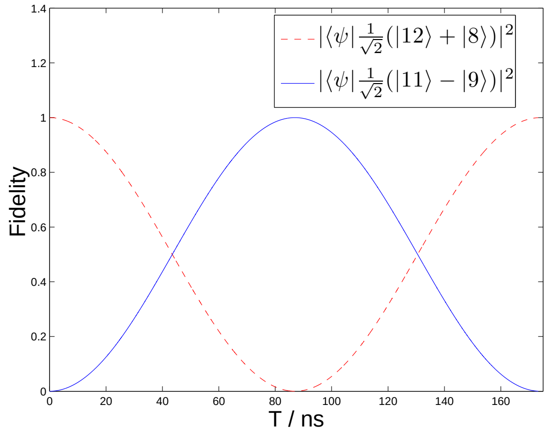

FIG. 3: Shows that near the $\tilde{\omega}_0 = 7$ cancellation resonance, the transition rates $|12\rangle \leftrightarrow |11\rangle$ and $|8\rangle \leftrightarrow |9\rangle$ equalise, and we may transfer the coherences between the former to the latter, with a relative phase shift of π. We use $\omega_1 = 200$ MHz.

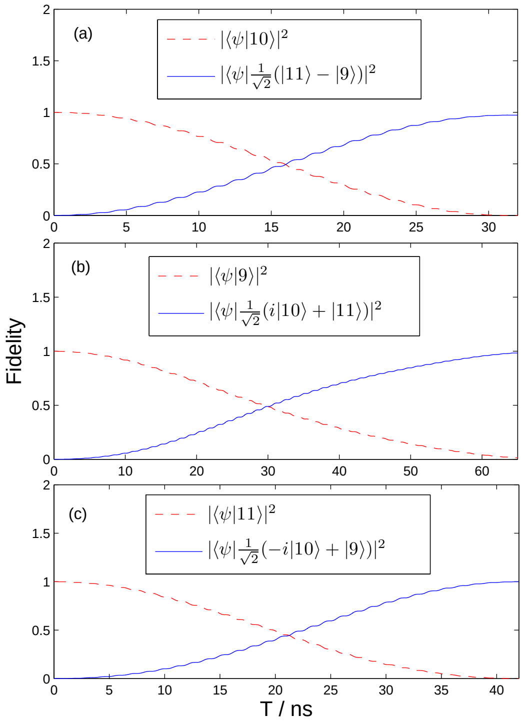

FIG. 4: Shows that at the $\tilde{\omega}_0 = 5$ resonance, second order, two-photon transitions may be exploited since $\omega(10-9) \simeq \omega(11-10)$ [15]. A linear oscillating microwave field of strength $\omega_1 = 200$ MHz is used. **(a)** shows that driving at resonance prepares $|10\rangle \rightarrow \frac{1}{\sqrt{2}}(|11\rangle - |9\rangle)$. The process is very sensitive to detuning from resonance. **(b)** and **(c)** illustrate how slight detuning of the microwave frequency may be used to prepare other superpositions such as $|9\rangle \rightarrow \frac{1}{\sqrt{2}}(i|10\rangle + |11\rangle)$ and $|11\rangle \rightarrow \frac{1}{\sqrt{2}}(-i|10\rangle + |9\rangle)$.

leaving only the ϵ_{-5} term. Here $E_{-5} \approx -\frac{A}{4}$, so its eigenvalue lies almost exactly half-way between the $|\pm,-4\rangle$ state eigenvalues: states $|9\rangle$, $|11\rangle$ have energies $E_{\pm} \approx E_{-5} \pm R_{-4}$ [15]. This gives the striking feature at 2.3 GHz in Fig.2(b) where the $|10\rangle \leftrightarrow |9\rangle$ and $|11\rangle \leftrightarrow |10\rangle$ lines coincide and where an EPR pulse would simultaneously generate coherences between state $|10\rangle$ and *both* states $|11\rangle$ and $|9\rangle$. In effect one may use two-photon, second order processes to transfer population between states $|9\rangle$ and $|11\rangle$ (recall that simultaneous spin flips are forbidden for isotropic hyperfine coupling). Fig.4 illustrates this.

F. Analogy with "exact cancellation"

Exact cancellation is a widely used "trick" in ESEEM spectroscopy. A coupled nuclear-electronic system with anisotropic hyperfine coupling, which is weak compared with electron spin frequencies (on the MHz scale rather than GHz scale), has a rotating frame Hamiltonian [12]:

$$\hat{H}_0 = \Omega_s \hat{S}_z + \omega_I \hat{I}_z + A\hat{S}_z \otimes \hat{I}_z + B\hat{S}_z \otimes \hat{I}_x. \tag{18}$$

Here $\Omega_s = \omega_0 - \omega$ is the detuning from the external driving field and $\omega_I = \delta\omega_0$ is the nuclear Zeeman frequency. At resonance, $\Omega_s = 0$. As the hyperfine terms are weak, terms like $\hat{S}_x \otimes \hat{I}_x + \hat{S}_y \otimes \hat{I}_y$ are averaged out by the rapidly oscillating (microwave) driving. The remaining Hamiltonian $\omega_I \hat{I}_z + A\hat{S}_z \otimes \hat{I}_z + B\hat{S}_z \otimes \hat{I}_x$ conserves m_s. For a spin $S = \frac{1}{2}, I = \frac{1}{2}$ system like Si:P, the Hamiltonian decouples into two separate 2×2 Hamiltonians $\hat{H}_{m_s=\pm\frac{1}{2}}$. In the $m_s = +\frac{1}{2}$ subspace,

$$\hat{H}_{m_s=+\frac{1}{2}} = \frac{1}{2}(\omega_I + \frac{A}{2})\sigma_z + \frac{B}{2}\sigma_x \tag{19}$$

where the Pauli matrices are defined relative to the basis $|m_s\rangle \otimes |m_I\rangle = |+\frac{1}{2}\rangle \otimes |\pm\frac{1}{2}\rangle$ while in the $m_s = -\frac{1}{2}$ subspace:

$$\hat{H}_{m_s=-\frac{1}{2}} = \frac{1}{2}(\omega_I - \frac{A}{2})\sigma_z + \frac{B}{2}\sigma_x \tag{20}$$

where the Pauli matrices are defined relative to the basis $|m_s\rangle \otimes |m_I\rangle = |-\frac{1}{2}\rangle \otimes |\pm\frac{1}{2}\rangle$. It is easy to see from Eq.(20) that if

$$\omega_I = \frac{A}{2} \tag{21}$$

only the $\frac{B}{2}\sigma_x$ term remains. This is the "exact cancellation" condition. While reminiscent of hyperfine cancellations resonances, there are key differences, other than the obvious one that the former occur as a series when $m = -\tilde{\omega}_0$ in Eq.(5), while the "exact cancellation" occurs at a single magnetic field. In particular, since the EPR cancellation resonances of Eq.(5) affect both nuclear and electron spins, at $m = -\tilde{\omega}_0$, the eigenstates assume "Bell-like" form:

$$|\Psi^{\pm}\rangle = \frac{1}{\sqrt{2}}\left(|-\frac{1}{2}\rangle_e \otimes |m+\frac{1}{2}\rangle_n \pm |+\frac{1}{2}\rangle_e \otimes |m-\frac{1}{2}\rangle_n\right) \tag{22}$$

where the e, n subscripts have been added for clarity, to indicate the electronic and nuclear states respectively. In contrast, for exact cancellation, they give superpositions of nuclear spin states only:

$$|\Psi\rangle = \frac{1}{\sqrt{2}}|-\frac{1}{2}\rangle_e \otimes \left(|+\frac{1}{2}\rangle_n \pm |-\frac{1}{2}\rangle_n\right), \tag{23}$$

which still permits interesting manipulations of the nuclear spin states [16].

Note that, while exact cancellation eliminates the full Ising term $A\hat{S}_z \otimes \hat{I}_z$, the EPR cancellation resonance eliminates only the non-isotropic part. In fact the EPR cancellation resonances result in a variety of different types of resonances. As discussed below, the $\omega_0 = 7A$ resonance does not cancel the hyperfine coupling at all; it equalizes the Bloch vector of the states in adjacent m-subspaces producing another effect (the "cancellation" label is in this case applied in a somewhat different sense).

EPR cancellation resonances are in practice a much stronger effect than exact cancellation: decohering and perturbing effects of interest in quantum information predominantly affect the electronic spins, not the nuclear spins. Exact cancellation appears in the rotating frame Hamiltonian (which contains only terms of order MHz). It will not survive perturbations approaching the GHz energy scale. The cancellation resonances, on the other hand, arise in the full Hamiltonian, eliminate large electronic terms and can potentially thus reduce the system's sensitivity to major sources of broadening and decoherence.

It is valuable to recall a major reason why the "exact cancellation" regime is so widely exploited in spectroscopic studies. In systems with anisotropic coupling, the spectra depend on the relative orientation of the coupling tensor and external field. Thus for powder spectra, which necessarily average over many orientations, very broad spectral features result. At exact cancellation, the simplification of the Hamiltonian is dramatically signalled by ultra-narrow spectral lines [12].

III. SI:BI AS A TWO-QUBIT SYSTEM

A. Basis states

The adiabatic eigenstates of the well-studied 4-state $S = 1/2$, $I = 1/2$ Si:P system can be mapped onto a two-qubit computational basis:

Adiabatic state	high-field state	logical qubit
$\|4\rangle$	$\|+\frac{1}{2}, +\frac{1}{2}\rangle$	$\|1_e 1_n\rangle$
$\|3\rangle$	$\|+\frac{1}{2}, -\frac{1}{2}\rangle$	$\|1_e 0_n\rangle$
$\|1\rangle$	$\|-\frac{1}{2}, +\frac{1}{2}\rangle$	$\|0_e 1_n\rangle$
$\|2\rangle$	$\|-\frac{1}{2}, -\frac{1}{2}\rangle$	$\|0_e 0_n\rangle$

With a 20-eigenstate state-space, the Si:Bi spectrum is considerably more complex. However, we can identify a natural subset of 4 states (states $|9\rangle, |10\rangle, |11\rangle$ and $|12\rangle$), which represents an effective coupled two–qubit analogue. As hyperpolarization initialises the spins in state $|10\rangle$ [6] and this state has both the electron and nuclear spins fully anti-aligned with the magnetic field, although it is not the ground state, it can be identified with the $|0_e 0_n\rangle$ state. The other states – just as in the Si:P case – are related to it by adding a single quantum of spin to one or both qubits:

For both systems, there are in principle 4 transitions which would account for all possible individual qubit operations, as listed in Table I. We show below that for Si:Bi, all single qubit operations are EPR-allowed for $B \lesssim 0.6$ T. For Si:P, only the electronic qubit-flips (the first two) are EPR-allowed; nuclear rotations require much slower, μs, NMR transitions. Measurement of the qubits in the computational basis has to be performed at high fields, where the adiabatic logical qubit coincides with the electron and nuclear spin states. All simultaneous nuclear and electronic qubit flips are forbidden for systems with isotropic hyperfine coupling A including both Si:P and Si:Bi. We note that, in spin-systems with "exact cancellation" and anisotropic A, the $A\hat{I}_x \otimes \hat{S}_z$ coupling does permit simultaneous nuclear-electronic qubit flips. These were recently shown for the organic molecule malonic acid [16]; the disadvantage here is that single nuclear qubit rotations (essential for quantum computation) are not EPR-allowed.

Adiabatic state	high-field state	logical qubit
$\|12\rangle$	$\|+\frac{1}{2}, -3\frac{1}{2}\rangle$	$\|1_e 1_n\rangle$
$\|11\rangle$	$\|+\frac{1}{2}, -4\frac{1}{2}\rangle$	$\|1_e 0_n\rangle$
$\|9\rangle$	$\|-\frac{1}{2}, -3\frac{1}{2}\rangle$	$\|0_e 1_n\rangle$
$\|10\rangle$	$\|-\frac{1}{2}, -4\frac{1}{2}\rangle$	$\|0_e 0_n\rangle$

Controlled operation	Si:P transitions	Si:Bi transitions
$\hat{R}_{\underline{v}}(\theta)_e \otimes \|0\rangle\langle 0\|_n$	$\boldsymbol{\omega_{3-2}}$	$\boldsymbol{\omega_{11-10}}$
$\hat{R}_{\underline{v}}(\theta)_e \otimes \|1\rangle\langle 1\|_n$	$\boldsymbol{\omega_{4-1}}$	$\boldsymbol{\omega_{12-9}}$
$\|0\rangle\langle 0\|_e \otimes \hat{R}_{\underline{v}}(\theta)_n$	ω_{2-1}	$\boldsymbol{\omega_{10-9}}$
$\|1\rangle\langle 1\|_e \otimes \hat{R}_{\underline{v}}(\theta)_n$	ω_{4-3}	$\boldsymbol{\omega_{12-11}}$

TABLE I: conditional single-qubit rotations of angle θ about vector $\underline{v}$ in the Bloch sphere, denoted $\hat{R}_{\underline{v}}(\theta)$, and corresponding transition frequencies. Frequencies in boldface correspond to qubit operations which are EPR-allowed at $B = 0.1 - 0.6$ T; i.e. they require only fast (ns) EPR pulses. All four EPR operations are possible for Si:Bi, whereas for Si:P nuclear qubit operations require slow (μs) NMR pulses. This scheme allows for cheap, controlled qubit operations, whereas single qubit operations would require twice the number of pulses.

B. Universal set of quantum gates

It is known that for universal quantum computation it suffices to be able to perform arbitrary single qubit rotations and a two-qubit gate such as the CNOT [17]. We now show how we may exploit the strong hyperfine interaction of the Si:Bi system to achieve this using only EPR pulses.

Control of the electron spins is facilitated by the Hamiltonian $\hat{H} = \hat{H}_0 + V_{x/y}(t)$ where $V_{x/y}(t) = \omega_1 \cos(\omega t)\hat{S}_{x/y}$ represents the external microwave frequency field oscillating along the x or y-axis. This may be written as:

$$\begin{aligned} V_{x/y}(t) &= \frac{\omega_1}{2}(\cos(\omega t)\hat{S}_{x/y} + \sin(\omega t)\hat{S}_{y/x}) + \\ &\quad \frac{\omega_1}{2}(\cos(\omega t)\hat{S}_{x/y} - \sin(\omega t)\hat{S}_{y/x}) \qquad (24) \end{aligned}$$

We label the first component the right handed (RH), and the second term the left handed (LH) rotating fields. In the rotating frame between two eigenstates $|e\rangle$ and $|g\rangle$ which satisfy the selection rule $\langle e|\hat{S}_{x/y}|g\rangle = \eta > 0$, the Liouville-von Neumann equation for the reduced two-level system is:

$$\frac{d\tilde{\rho}(t)}{dt} = i\frac{\omega_1 \eta}{4}[\tilde{\rho}(t), \hat{\sigma}_{x/y}]. \qquad (25)$$

if $\omega_1 << \Omega_0$ where $\Omega_0 = |\lambda_e - \lambda_g|$ is the energy difference between the two eigenstates. For most possible transitions, η is positive and the resonance condition is satisfied by the RH component of the oscillating microwave field. But for transitions $|-, m\rangle \leftrightarrow |-, m-1\rangle$, $\eta = a_m^- b_{m-1}^- < 0$ and as such it is brought to resonance by the LH component of the microwave field. This feature, which is explained in more detail in Appendix.A, may aid in selective qubit manipulation as will be explained below.

The transition strengths given in Eqs.(12), (13) and (14) are given by $|\eta|^2$. Eq.(25) shows that the qubit rotation speed, given a fixed microwave field strength, is determined by the mixing factor η. As $B \to \infty$, $\eta \to 1$ for high-field EPR transitions, and $\eta \to 0$ for high-field NMR transitions. At magnetic fields where $A \sim B$, however, mixing occurs and η will be appreciable for said transitions.

At the $m = -4$ cancellation resonance, established when $\omega_0 = 4A$ ($B = 0.21$ T), $|\eta|$ for both nuclear and electronic qubit operations become exactly equal: this is simple to verify from Eqs.(12)-(14) by setting $\theta_{-5} = 0$ and $\theta_{-4} = \pi/2$. We show numerically in Fig.5(a)-(b) that this means a π pulse on the nuclear qubit becomes as short as on the electronic one. For higher fields, however, η for nuclear qubit flips falls off as $1/B$.

The EPR pulses at our disposal allow us to perform controlled single qubit unitaries $R_{\underline{v}}(\theta)$ where $\underline{v}$ lies in the $x-y$ plane. Two orthogonal Paulis suffice to generate arbitrary single-qubit unitaries [18] using at most three pulses, and we may construct the controlled $\hat{\sigma}_z$ and Hadamard gates by these pulse sequences:

$$\begin{aligned} \hat{\sigma}_z &= e^{i\frac{3\pi}{2}} e^{i\frac{\pi}{2}\hat{\sigma}_y} e^{i\frac{\pi}{2}\hat{\sigma}_x} \\ H := \frac{1}{\sqrt{2}}(\hat{\sigma}_x + \hat{\sigma}_z) &= e^{i\frac{3\pi}{2}} e^{i\frac{\pi}{2}\hat{\sigma}_x} e^{i\frac{3\pi}{4}\hat{\sigma}_y} e^{i\pi\hat{\sigma}_x} \end{aligned} \tag{26}$$

The possible controlled operations are shown in Table I. Single-qubit gates would require us to repeat the set of controlled EPR pulses for both the controlling qubit basis states, and as such would require twice the time.

C. Selective qubit gates

Consider the initial state $|\psi\rangle = \frac{1}{\sqrt{2}}(|1_e 1_n\rangle + |0_e 1_n\rangle)$. If we wanted to perform a CNOT gate on this state, with the electron qubit as the control, we may choose to use the transition frequency ω_{12-11} as dictated by Table I. However, this frequency is only a few MHz different from that of ω_{9-8}, and a short pulse of ~ 50 ns would have a bandwidth of ~ 20 MHz which would also drive the transition between states $|9\rangle$ and $|8\rangle$, and thereby effect a noise operation on our qubits. There are two strategies to overcome this complication:

1. by tuning the microwave frequency to be exactly between the wanted and unwanted transition frequencies, we ensure they both suffer the same effective $\omega_1' = \omega_1 \mathrm{sinc}(\frac{T}{2}(\Omega^{12\leftrightarrow 11} + \Omega^{9\leftrightarrow 8}))$, where T is the pulse duration and Ω is the transition frequency, such that the only variable affecting the two transition rates would be the mixing factor η. Near the $m = -4$ cancellation resonance at $B = 0.22$ T we get $\frac{|\eta_{12\to 11}|}{|\eta_{9\to 8}|} = 5/4$. This ensures that at time $t = \frac{10\pi}{\omega_1' |\eta_{12\to 11}|}$, we perform the operation:

   $$\frac{1}{\sqrt{2}}\left(-i\hat{\sigma}_x^n |1_e 1_n\rangle + \mathbb{1}|0_e 1_n\rangle\right) = \frac{1}{\sqrt{2}}\left(-i|1_e 0_n\rangle + |0_e 1_n\rangle\right). \tag{27}$$

   This is shown numerically in Fig.5(c).

2. The transition $|12\rangle \to |11\rangle$ utilises the RH component of the microwave field, whereas the $|9\rangle \to |8\rangle$ transition uses the LH one. By generating a RH circularly polarised microwave field, we would be able to select for the desired transition, as shown in Fig.5(d).

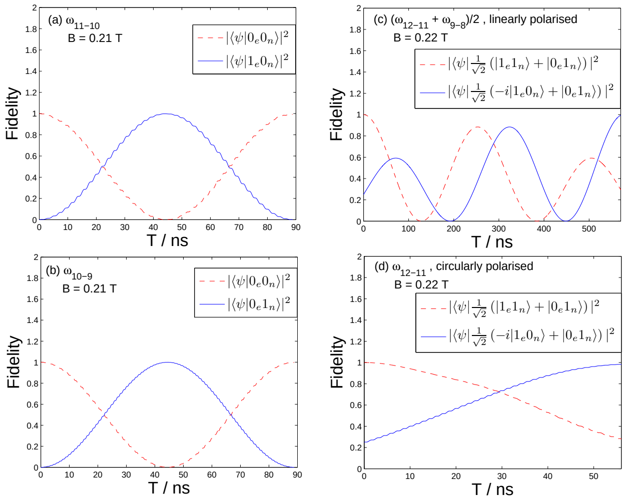

FIG. 5: **(a)** and **(b)** show Rabi oscillations utilising a linearly oscillating microwave field of strength $\omega_1/2\pi = 200$ MHz. For $B = 0.21$ T, the time taken for the electron qubit flip $|0_e 0_n\rangle \to |1_e 0_n\rangle$ is identical to that for the nuclear qubit flip $|0_e 0_n\rangle \to |0_e 1_n\rangle$. **(c)** and **(d)** show selective nuclear qubit flips, and have microwave fields of strength $\omega_1/2\pi = 100$ MHz. This is because the energy difference between the eigenstates is smaller than in the previous two cases and ω_1 must remain perturbative. **(c)** Utilises a linearly oscillating microwave field, which is non-selective for short pulses. At $B = 0.22$ T the rotation speed ratio is $\frac{|\eta_{12\to 11}|}{|\eta_{9\to 8}|} = \frac{5}{4}$. A 5π rotation of the nuclear qubit corresponds to a 4π rotation of the unwanted $|9\rangle \to |8\rangle$ transition. In **(d)** we use a RH circularly polarised microwave field, which selects for the desired conditional nuclear qubit rotation, and is much more efficient than the linearly polarised case.

D. Scaling with controllable Heisenberg interaction

So far we have only described how to perform two-qubit gates in a single site of Si:Bi (or any other nuclear-electronic system obeying the same Hamiltonian and with a large enough hyperfine exchange term). This is very limited, however, and we need to be able to scale the system so as to incorporate arbitrarily large numbers of qubits. With Si:Bi, the possibility does exist to further utilise the 20 dimensional Hilbert space, which would provide a maximum of 4 qubits. This is, however, not scalable, and we will still be limited to just 4 qubits as we cannot create more energy levels within the single-site Si:Bi system. The only feasible option that remains, is to have spatially separated Si:Bi centers, between which we can establish an interaction. The original Kane proposal [1] envisaged a Heisenberg interaction between nearest neighbour electrons which could be controlled via electric fields. This interaction has the form:

$$\hat{H}_{int} = J\hat{\mathbf{S}}^i.\hat{\mathbf{S}}^{i+1} \tag{28}$$

As shown by [19] such an interaction can be used to produce a $\sqrt{\text{SWAP}}$ gate:

$$\sqrt{\text{SWAP}} = e^{i\frac{\pi}{8}}e^{-i\frac{\hat{H}_{int}}{J}\frac{\pi}{2}} \tag{29}$$

Using two such gates, together with single-qubit unitaries, we can establish a CZ gate between the electrons:

$$CZ^{12} = e^{i\frac{\pi}{2}}\left(e^{-i\hat{\sigma}_z^1\frac{\pi}{4}} \otimes e^{i\hat{\sigma}_z^2\frac{\pi}{4}}\right)\sqrt{\text{SWAP}}e^{-i\hat{\sigma}_z^1\frac{\pi}{2}}\sqrt{\text{SWAP}} \tag{30}$$

As stated in previous sections, we cannot perform rotations about the z axis of the Bloch sphere directly, but we can use our EPR pulses about the x and y axes to produce the required single-qubit unitaries.

$$e^{-i\hat{\sigma}_z^1\frac{\pi}{4}} = e^{i\pi}e^{-i\hat{\sigma}_y^1\frac{3\pi}{4}}e^{-i\hat{\sigma}_x^1\frac{\pi}{4}}e^{-i\hat{\sigma}_y^1\frac{\pi}{4}} \tag{31}$$

The CZ gate can be turned into a CNOT gate by simply applying a Hadamard on the target qubit before and after the application of the CZ. Such an interaction affects the electron spin basis states, and not the adiabatic basis states to which we have designated our logical qubits. Therefore, we must apply our electronic two-qubit gates in the high-field limit where mixing is suppressed, and where there is a high fidelity between the adiabatic basis and spin basis. A consequence of this is that the energy difference between different eigenstates will be very large and, as is well known [20], if $|E_i - E_{i+1}| >> J$, the Heisenberg interaction between the two effectively becomes an Ising interaction $J\hat{S}_z^1 \otimes \hat{S}_z^2$. To use the above scheme of producing entangling two-qubit gates between all 4 eigenstates in each of the two adjacent sites, we would have to establish a very strong J.

Alternatively, we can set B_i and B_{i+1} to be sufficiently different, and J small enough, such that we only get an Ising interaction between all relevant eigenstates. It is in fact easier to produce the CZ and CNOT gates with an Ising interaction, as it only requires one exchange operation and not two as in the case of the Heisenberg interaction [21, 22].

$$CZ^{12} = e^{-i\frac{\pi}{4}}\left(e^{i\hat{\sigma}_z^1\frac{\pi}{4}} \otimes e^{i\hat{\sigma}_z^2\frac{\pi}{4}}\right)e^{-i\hat{S}_z^1\otimes\hat{S}_z^2\pi} \tag{32}$$

IV. DECOHERENCE FROM TEMPORAL MAGNETIC FIELD FLUCTUATIONS

For practical quantum information processing in silicon, the substance would need to be purified so as not to contain any ^{29}Si such that no decoherence would result due to spin-bath dynamics. Temperatures would also be maintained at low levels so as to minimise the phonon-bath induced decoherence. Here, we wish to employ a phenomenological model of decoherence for nuclear-electronic systems, resulting only from stochastic magnetic-field fluctuations. Taking the Hamiltonian from Eq.(1) and adding to it a perturbative term involving independent temporal magnetic-field fluctuations in all three spatial dimensions (all of which take a Gaussian distribution with mean 0 and variance α_n^2) gives, in the interaction picture:

$$\tilde{H}(t) = \sum_{n=1}^{3}\omega_n(t)\tilde{S}_n(t) + \omega_n(t)\delta\tilde{I}_n(t) \tag{33}$$

We may ignore the nuclear term as its effects will be negligible. We then follow the standard procedure of deriving a Born-Markov master equation [25]:

$$\frac{d}{dt}\langle\rho(t)\rangle = i\left[\langle\rho(t)\rangle, \hat{H}_0\right] + \alpha_n^2\sum_{n=1}^{3}\sum_{\Omega}e^{-f_n\Omega^2} \times \left(\hat{S}_n^\dagger(\Omega)\langle\rho(t)\rangle\hat{S}_n(\Omega) - \frac{1}{2}\left[\langle\rho(t)\rangle, \hat{S}_n^\dagger(\Omega)\hat{S}_n(\Omega)\right]_+\right) \tag{34}$$

where $\hat{S}_n(\Omega)$ are the electron spin operators in the eigenbasis of $\hat{H}_0$, Ω is the energy difference between two such eigenstates, and $f_n = (\frac{dB_n}{dt})^{-1}$. $\langle\rho(t)\rangle$ is defined as the density operator of the coupled nuclear-electronic system, averaged over either an ensemble of such systems, or repeated experiments on a single system. Further details for the derivation of Eq.(34) can be found in Appendix B.

The rate term $e^{-f_n\Omega^2}$ imposes the results of the adiabatic theorem into our master equation. The quantitative condition for adiabatic evolution is often cited as [26]

$$\left|\frac{\langle\phi|\dot{H}(t)|\psi\rangle}{(E_\phi - E_\psi)^2}\right| << 1. \tag{35}$$

For the model described here, this translates to

$$\left|\langle\phi|\hat{S}_n|\psi\rangle\frac{\frac{dB_n}{dt}}{(E_\phi - E_\psi)^2}\right| = \left|\langle\phi|\hat{S}_n|\psi\rangle\right|\frac{1}{f_n\Omega^2} << 1 \tag{36}$$

which means that, in the case of $\left|\langle\phi|\hat{S}_n|\psi\rangle\right| > 0$, if the magnetic field is fluctuating sufficiently slowly, the probability of transition between eigenstates $|\psi\rangle$ and $|\phi\rangle$ becomes vanishingly small.

Since we have made the rotating wave (or secular) approximation, and are only interested in the interaction picture dynamics of our system, we may drop the Hamiltonian commutator in Eq.(34), leaving only the dissipator term. We are now equipped with the tools to address decoherence in our quantum system. We may model our gates as ideal unitaries that can prepare some superposition $|\psi\rangle = a|e\rangle + b|g\rangle$ between the adiabatic basis states $|e\rangle$ and $|g\rangle$, which is then decohered according to our noise model. The dephasing and depolarising rates are determined by applying our master equation and measuring the rate that the observables

$$\sqrt{tr(\sigma_x\tilde{\rho}(t))^2 + tr(\sigma_y\tilde{\rho}(t))^2} \tag{37}$$

and

$$tr(\sigma_z\tilde{\rho}(t)) \tag{38}$$

decay respectively. In the cases that these decay exponentially, we may characterise the dephasing and depolarising times by T_2 and T_1 respectively, which are the inverse of the decay rates. Such times are measured in EPR experiments [23, 24]. The Pauli matrices denoted here are in the eigen-basis of the reduced two-level system in question. We will study two types of noise; Z noise and X noise, so named due to Gaussian magnetic-field fluctuations in the z-axis and x-axis respectively. Throughout this section, when an adiabatic state is designated with m, it is implied that $|m| < (I+\frac{1}{2})$, and states where $m = \pm(I+\frac{1}{2})$ are explicitly designated.

A. Z noise

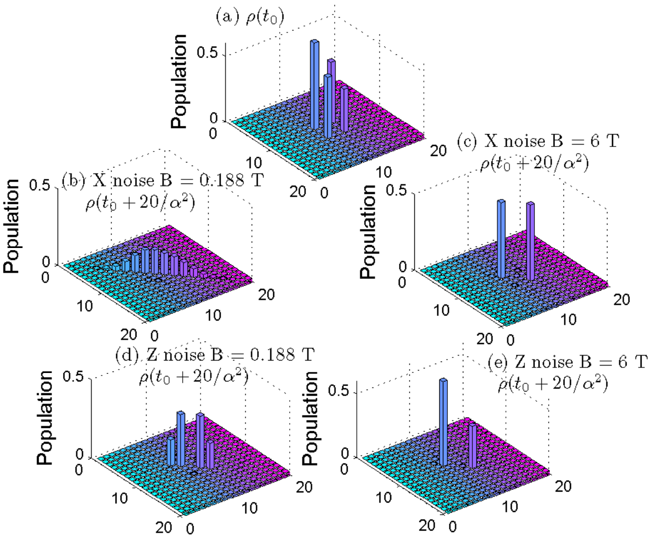

FIG. 6: Shows the change in density operator elements of $|\psi\rangle = \frac{2}{\sqrt{3}}|9\rangle + \frac{1}{\sqrt{3}}|12\rangle$ after a period of $20/\alpha^2$, given diabatic Gaussian noise of variance α^2, at two field regimes: the frequency minima of $B = 0.188$ T, and $B = 6$ T . (a) Population of ρ in the eigen-basis of $\hat{H}_0$ at time t_0. (b) - (c) show the effect of B on the properties of X noise. (b) Near the frequency minima, X noise couples every part of the full Hilbert space, and effects a depolarising channel for the full system, ultimately resulting in $\frac{1}{20}\mathbb{1}$. (c) At $B = 6$ T, X noise decouples states $|+,m\rangle, |-,m-1\rangle$ from the rest of the Hilbert space, and effects a depolarising channel in that subspace only. (d) - (e) show the effect of B on the properties of Z noise. Z noise conserves angular momentum and hence keeps to the 4-dimensional Hilbert space of $m = -3, m-1 = -4$. (d) shows that at the frequency minima of $B = 0.188$ T, Z noise effects independent depolarising channels for each m subspace. As a result, the population of states $|12\rangle$ and $|9\rangle$ equalise with those of states $|8\rangle$ and $|11\rangle$ respectively.(e) shows that at $B = 6$ T, $\langle +,m|\hat{S}_z|-,m\rangle \sim 0$ and we simply get a dephasing channel for the $|+,m\rangle, |-,m-1\rangle$ subspace.

Given Z noise, we may consider our system as a decoupled four-level system with sub Hamiltonian:

$$H_{sub} = (\Omega_m\sigma_x + \Delta_m\sigma_z) \oplus (\Omega_{m-1}\sigma_x + \Delta_{m-1}\sigma_z) \tag{39}$$

ignoring any identity terms. This is possible as there will be no transfer of population to other components of the Hilbert space. We may write $\hat{S}_z$ in the adiabatic basis $\{|+,m\rangle, |-,m\rangle, |+,m-1\rangle, |-,m-1\rangle\}$:

$$\begin{pmatrix} \cos(\theta_m) & -\sin(\theta_m) & 0 & 0 \\ -\sin(\theta_m) & -\cos(\theta_m) & 0 & 0 \\ 0 & 0 & \cos(\theta_{m-1}) & -\sin(\theta_{m-1}) \\ 0 & 0 & -\sin(\theta_{m-1}) & -\cos(\theta_{m-1}) \end{pmatrix} \tag{40}$$

Substituting this into Eq.(34) gives

$$\begin{aligned} \frac{d}{dt}\langle\rho(t)\rangle &= \sum_{n=m-1}^{m} i\left[\langle\rho(t)\rangle, \frac{\Omega_n}{2}\hat{\sigma}_z^n\right] + \\ &\frac{\alpha^2}{4}\cos^2(\theta_n)(\hat{\sigma}_z^n\langle\tilde{\rho}(t)\rangle\hat{\sigma}_z^n - \langle\tilde{\rho}(t)\rangle) + \\ &\frac{\alpha^2}{4}e^{-f\Omega^2}\sin^2(\theta_n)\times \\ &(|+,n\rangle\langle -,n|\langle\tilde{\rho}(t)\rangle|-,n\rangle\langle +,n| - \\ &|+,n\rangle\langle -,n||-,n\rangle\langle +,n|\langle\tilde{\rho}(t)\rangle + H.C.). \end{aligned} \tag{41}$$

In the infinite-field limit our EPR local unitaries can only create superpositions $a|+,m\rangle + b|-,m-1\rangle$. As the noise operator takes the form $\hat{\sigma}_z^m \oplus \hat{\sigma}_z^{m-1}$ in this regime, this superposition may be considered to exist as a decoupled two-level system. We may therefore solve Eq.(41) (for the two-level subspace in question) analytically:

$$e^{\mathcal{L}t}\tilde{\rho}(t_0) = \frac{1}{2}\left(1+e^{-\frac{t}{T_2}}\right)\tilde{\rho}(t_0) + \frac{1}{2}\left(1-e^{-\frac{t}{T_2}}\right)\hat{\sigma}_z\tilde{\rho}(t_0)\hat{\sigma}_z. \tag{42}$$

where $\mathcal{L}$ is the Liouville superoperator, whose action on ρ is given by Eq.(41). This is simply the dephasing channel for a spin 1/2 particle [18]:

$$\mathcal{E}(t)\circ\rho = (1-\lambda(t))\rho + \lambda(t)\hat{\sigma}_z\rho\hat{\sigma}_z \tag{43}$$

with probability $\lambda(t)$ of performing a $\hat{\sigma}_z$ operation under conjugation. Here, $\lambda(t) = \frac{1-e^{-\frac{t}{T2}}}{2}$ with a T_2 time of $2/\alpha^2$. This is illustrated by Fig.6(e), where only the off-diagonal elements of $\rho(t_0)$, as shown in Fig.6(a), decay. At low fields however, $\langle +,m|\hat{S}_z|-,m\rangle > 0$ and we cannot ignore the exchange term in Eq.(41). In this case, we may use the 4-dimensional Bloch vector representation of our density operator:

$$\rho(t) = \frac{1}{4}\left(\sum_{i,j=0}^{3} n_{ij}(t)\hat{\sigma}_i\otimes\hat{\sigma}_j\right),\ n_{00}(t) = 1 \tag{44}$$

It is possible to map the dynamics of the density operator to that of the Bloch vector [27] as

$$\frac{d\underline{\mathbf{n}}(t)}{dt} = \mathcal{L}\underline{\mathbf{n}}(t). \tag{45}$$

For the stated problem the 16 simultaneous differential equations can be solved to obtain analytic expressions for the dephasing and depolarising rates. Alternatively, by decomposing $\underline{\mathbf{n}}(t)$ in the eigenbasis of $\mathcal{L}$, denoted $\underline{\mathbf{n}}_l$ with generally complex eigenvalues λ_l, we may represent the dynamics of the Bloch vector as

$$\underline{\mathbf{n}}(t) = \sum_{l=0}^{15} c_l \underline{\mathbf{n}}_l e^{t\lambda_l}. \tag{46}$$

where c_l are determined by the initial conditions. It is the real component of the eigenvalues which leads to decay in population of the eigenstate. The infinite time state is therefore a superposition of eigenstates $\underline{\mathbf{n}}_l$ such that $Re(\lambda_l) = 0$.

1. Adiabatic Z noise

Here we may set $f \to \infty \implies e^{-f\Omega^2} = 0$ for $\Omega^2 > 0$. There will be no depolarisation in this case, and we may only have pure dephasing. For superpositions of type $a|+, m\rangle + b|-, m-1\rangle$, the dephasing rate, parameterised as the decay of the off-diagonal elements of the subspace in question, is given by

$$\frac{1}{T_2} = \frac{\alpha^2}{8}(\cos(\theta_m) + \cos(\theta_{m-1}))^2. \tag{47}$$

When $\cos(\theta_m) = -\cos(\theta_{m-1})$, which is satisfied at the frequency minima, dephasing due to $\hat{S}_z$ is completely removed.

For superpositions of type $a|\pm, m\rangle + b|\pm, m-1\rangle$, the dephasing rate is given by

$$\frac{1}{T_2} = \frac{\alpha^2}{8}(\cos(\theta_m) - \cos(\theta_{m-1}))^2. \tag{48}$$

Here there are two regions where the $\hat{S}_z$ caused dephasing is removed; when $\cos(\theta_m) = \cos(\theta_{m-1})$ which occurs at the frequency maxima, and at the high-field limit where $\cos(\theta_m) = \cos(\theta_{m-1}) = 1 \ \forall \ m$, rendering such transitions as only NMR allowed.

For superpositions of type $a|\pm, \pm(I + \frac{1}{2})\rangle + b|\pm, m\rangle$ the dephasing rate is given by

$$\frac{1}{T_2} = \frac{\alpha^2}{2}\sin\left(\frac{\theta_m}{2}\right)^4 \tag{49}$$

which reaches its minimal value of 0 as $B \to \infty$, whereas for superpositions of type $a|\pm, \pm(I + \frac{1}{2})\rangle + b|\mp, m\rangle$ it is given by

$$\frac{1}{T_2} = \frac{\alpha^2}{2}\cos\left(\frac{\theta_m}{2}\right)^4 \tag{50}$$

which reaches its minimal value (which is generally greater than 0) at $B = 0$ T. The steady state solution for adiabatic Z noise is given by

$$\underline{\mathbf{n}}(\infty) = \mathbb{1} \otimes \mathbb{1} + c_1 \mathbb{1} \otimes \hat{\sigma}_z + c_2 \hat{\sigma}_z \otimes \mathbb{1} + c_3 \hat{\sigma}_z \otimes \hat{\sigma}_z. \tag{51}$$

2. Diabatic Z noise

Here we may set $f \to 0 \implies e^{-f\Omega^2} = 1 \ \forall \ \Omega^2$. Solving the Bloch vector differential equations yields analytic expressions for the dephasing rates. For an initial superposition of $a|+, m\rangle + b|-, m-1\rangle$ this gives:

$$\frac{1}{T_2} = \frac{\alpha^2}{4}\left(\cos(\theta_m)\cos(\theta_{m-1}) + 1\right) \tag{52}$$

and for $a|\pm, m\rangle + b|\pm, m-1\rangle$:

$$\frac{1}{T_2} = \frac{\alpha^2}{4}\left(\cos(\theta_m)\cos(\theta_{m-1}) - 1\right). \tag{53}$$

Eq.(52) reaches a minimum value (hence giving the longest T_2 time) when $\cos(\theta_m) = -\cos(\theta_{m-1})$ i.e. at the frequency minima. Unlike the adiabatic Z noise case, this value does not reach 0, but rather reaches approximately half its maximal value at the high-field regime. Conversely, Eq.(53) reaches its maximal value when $\cos(\theta_m) = -\cos(\theta_{m-1})$, attaining approximately the same value as for Eq.(52) at this regime. Note that unlike the adiabatic case, there is no decoherence minimum at the frequency maxima; the decay rate simply vanishes as $B \to \infty$.

Because the exchange terms in Eq.(41) contribute to the dynamics for diabatic Z noise, there will also be depolarising noise in each m subspace, equalising the population in states $|\pm, m\rangle$. Fig.6(d) shows the effect of this depolarisation at the frequency minima. This depolarisation rate of each m subspace is given by:

$$\frac{1}{T_1} = \frac{\alpha^2}{2}\sin(\theta_m)^2. \tag{54}$$

which vanishes as $B \to \infty$, and maximises at the avoided crossing cancelation resonance. Given any superposition $\sqrt{P_g}|g\rangle + e^{i\phi}\sqrt{P_e}|e\rangle$, with states $|g\rangle$ and $|e\rangle$ each existing in a different m subspace, such that $E_e > E_g$, the depolarisation is given by:

$$tr(\sigma_z\tilde{\rho}(t)) = \frac{1}{2}P_e\left(1 + e^{-t/T_1^e}\right) - \frac{1}{2}P_g\left(1 + e^{-t/T_1^g}\right) \tag{55}$$

where $1/T_1^{g/e}$ is the depolarisation rate in the m subspace for $|g\rangle$ and $|e\rangle$, respectively. The steady state solution for diabatic Z noise given such superpositions is given by

$$\underline{\mathbf{n}}(\infty) = \mathbb{1} \otimes \mathbb{1} + c_1 \hat{\sigma}_z \otimes \mathbb{1} \tag{56}$$

where $c_1 \in [1, -1]$.

For superpositions of type $a|\pm, \pm(I + \frac{1}{2})\rangle + b|\pm, m\rangle$ the dephasing rate is given by

$$\frac{1}{T_2} = \frac{\alpha^2}{4}(1 - \cos(\theta_m)) \tag{57}$$

and for superpositions of type $a|\pm, \pm(I + \frac{1}{2})\rangle + b|\mp, m\rangle$ the dephasing rate is given by

$$\frac{1}{T_2} = \frac{\alpha^2}{4}(1 + \cos(\theta_m)). \tag{58}$$

The depolarisation rate can be calculated as in the previous case, using Eq.(55), and noting that one of $T_1^{g/e}$ is equal to ∞. The steady state solution for diabatic Z noise for such superpositions is given by

$$\underline{\mathbf{n}}(\infty) = \mathbb{1} \otimes \mathbb{1} + c_1 \hat{\sigma}_z \otimes \mathbb{1} + c_2 \mathbb{1} \otimes \hat{\sigma}_z. \qquad (59)$$

For diabatic Z noise, Fig.7 shows the analytical depolarisation and dephasing rates for subspace $m = -3, m-1 = -4$. Fig.8(a) shows the numerically calculated T2 times for all EPR lines depicted in Fig.2(b), whilst Fig.9(a) shows the numerically calculated depolarising times T1 in units of $2/\alpha^2$ for each m-subspace.

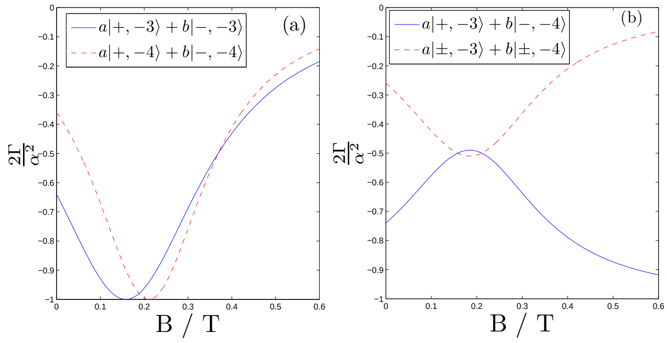

FIG. 7: The exponential decay rate given by Γ in units of $\alpha^2/2$ for diabatic Z noise driven (a) depolarisation and (b) dephasing. This is done in the 4 dimensional subspace of $m = -3, m-1 = -4$. (a) shows that in each subspace, the depolarisation rate maximises when $\theta_m = \pi/2$, or the avoided crossing cancelation resonances. (b) shows that at the high-field limit, the dephasing rate of $a|+,m\rangle + b|-,m-1\rangle$ is maximal, whilst that of $a|\pm,m\rangle + b|\pm,m-1\rangle$ becomes vanishingly small. These rates both approximately reach the value of 1/2 at the frequency minima.

B. X noise

X noise is less trivial, as it couples all components of the Hilbert space so we cannot consider a sub-Hamiltonian in isolation. Solving the resulting 400 Bloch equations (for Si:Bi) would be unfeasible, so only numerical calculations are given here. Furthermore, the adiabatic condition must be violated for X noise to have any effect, as there are no $\hat{S}_x(\Omega = 0)$ terms in Eq.(34). In the high-field limit the X noise operator will take the form of $\hat{\sigma}_x \otimes \mathbb{1}$ in the basis $\{|+,m\rangle, |-,m-1\rangle\}$. At such fields, as shown in Fig.6(c), an arbitrary superposition of $a|+,m\rangle + b|-,m-1\rangle$ suffers a two-level system depolarising channel. At low fields, however, the dissipation is not contained within the $m, m-1$ subspace, and as indicated by Fig.6(b) the system eventually decays to $\frac{1}{d}\mathbb{1}$.

For X noise, all dephasing is a result of the depolarising noise that is effected by the X noise operator, and as shown in Fig.8(b), at $B > 0.6$ T the dephasing time is $4/\alpha^2$ for all transitions. This value increases only slightly at magnetic fields smaller than the frequency minima for transitions involving $m < 0$.

Fig.9(b) shows the different forms of depolarising rates for X noise. At high magnetic fields, where the only non-vanishing matrix elements of the X noise operator are $\langle +,m|\hat{S}_x|-,m-1\rangle$, the depolarising noise follows an exponential decay. Under intermediate magnetic fields however, the dissipation follows a more complicated mechanism and the decay is better explained by a double exponential fit.

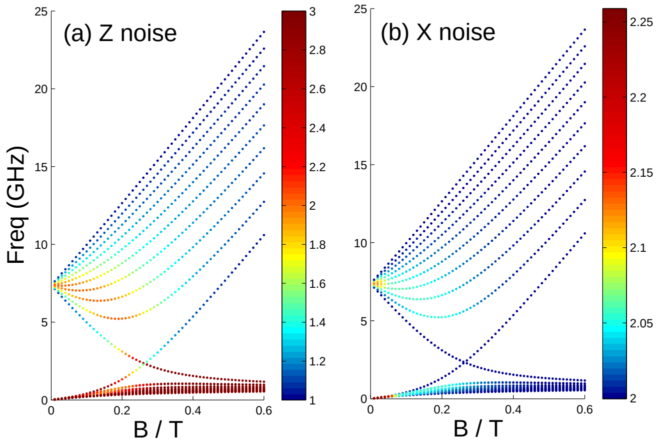

FIG. 8: Simulated dephasing times in units of $2/\alpha^2$ for diabatic (a) Z noise and (b) X noise. In (a) the superpositions $a|+,m\rangle + b|-,m-1\rangle$ have T_2 times of $2/\alpha^2$ at $B \gtrsim 0.6$ T, and approximately $4/\alpha^2$ at the frequency minima. Superpositions $a|\pm,m\rangle + b|\pm,m-1\rangle$ also have T_2 times of $4/\alpha^2$ at the frequency minima. However, as B increases, these become NMR transitions and will have T_2 times of $2/(\alpha^2\delta)$. The colour bar has been truncated after 3 to aid visibility. In (b), the T_2 time does not vary by much, and reaches its maximal points at fields less than the frequency minima.

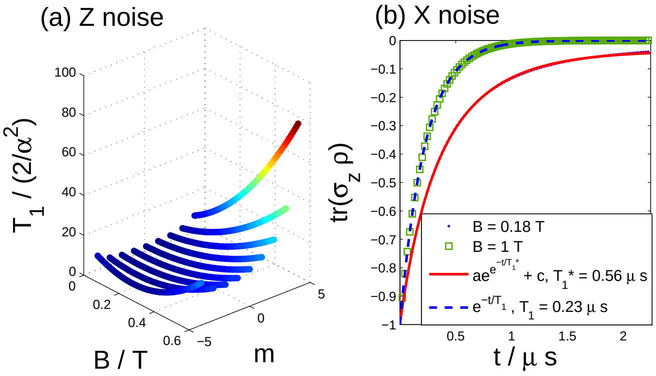

FIG. 9: Simulated depolarising times for diabatic Z and X noise with $\alpha^2 = 9$ MHz. (a) Given Z noise, the decay of $tr(\sigma_z \tilde{\rho}(t))$ within each m-subspace is always exponential. For $m \le 0$ the T_1 time reaches a minimum at the avoided crossing cancellation resonances. The T_1 time for subspace m and $m-1$ become identical at the frequency minima (b) Given X noise, the decay in the $|+,m\rangle$ $|-,m-1\rangle$ subspace follows an exponential curve at high magnetic fields, but at low magnetic fields such as the frequency minima, it follows a double exponential fit.

V. CONCLUSIONS

A coupled nuclear-electronic spin system with large A and $I \geq 1$ will give cancelation resonances at non vanishing magnetic fields. In the intermediate-field regime ($B \simeq 0.1 - 0.6$ T) the exceptionally large values of A and

I of Si:Bi generate a series of such cancellation resonances. Two eigenstates, with an EPR transition, which have a cancelation resonance will have two $\frac{df}{dB} = 0$ points in the spectrum; a frequency minimum and maximum. These points are associated with subtle and hereto unstudied effects: both line broadening and decoherence effects may be reduced. If the electronic and nuclear spins of Si:Bi are used as a coupled two-qubit system, the cancellation resonances allow a universal set of quantum gates to be performed with fast EPR microwave pulses, eliminating the need for slower radio frequency addressing of the nuclear qubit.

One scheme would envisage the following stages: (1) hyperpolarization of the sample into state $|10\rangle$ (in which the 2-qubit system is initialized as $|0\rangle_n|0\rangle_e$) at $B \approx 5$T (2) A magnetic field pulse (~ 10 T/ms, of duration lower than decoherence times) would reduce B to $\simeq 0.1$T (3) A series of EPR pulses would be carried out on the system in the low-field regime (4) As the magnetic pulse decays, the system is restored to the high-B limit, leaving it in the desired superposition of $|0\rangle_e|0\rangle_n, |1\rangle_e|1\rangle_n, |0\rangle_e|1\rangle_n$ and $|1\rangle_e|0\rangle_n$ basis states. (5) Turn on a Heisenberg exchange interaction between spatially separated bismuth sites to effect a two-qubit gate on the electron qubits. Thus, given the capability to rapidly ($\lesssim 1$ ms) switch from the high to intermediate-field regime, Si:Bi confers significant additional possibilities for quantum information processing relative to Si:P. We conclude that in particular the $m = -4$ cancellation resonance at 0.21 T may represent an "optimal working point" for quantum computation with Si:Bi for several reasons: (a) it is the point at which nuclear and electronic qubit flip times equalize (b) it provides $df/dB = 0$ points (c) it is associated with line narrowing. The other resonances provide a subset of these characteristics. The advantages of the $df/dB = 0$ points have been quantified relative to Gaussian noise: the Markovian model of decoherence presented here suggests longer dephasing times at the frequency minima given Gaussian temporal magnetic field fluctuations in the z-axis.

Acknowledgments

M. Hamed Mohammady acknowledges an EPSRC studentship, and Ahsan Nazir thanks Imperial College London and the EPSRC for financial support. Gavin Morley is supported by an 1851 Research Fellowship and the EPSRC COMPASSS grant. The authors would like to thank Dara P. S. McCutcheon for the insightful discussions that helped the development of the decoherence theory in this paper.

Appendix A: Selective rotations

Consider the coupled nuclear-electronic spin system in the eigenbasis of the Hamiltonian $\hat{H}_0$ given by Eq.(1). The electron spin operators in this basis are given by the unitary transformation

$$\hat{S}'_x = V^\dagger \hat{S}_x V \qquad \hat{S}'_y = V^\dagger \hat{S}_y V \tag{A1}$$

where V is a matrix whose i^{th} column is the i^{th} eigenvector of $\hat{H}_0$. We want to be able to isolate two eigenstates of this Hamiltonian, and perform unitary dynamics in that subspace. Tracing out all eigenvectors other than $|e\rangle$ and $|g\rangle$ gives

$$\begin{aligned}
(\hat{S}'_x)^{eg} &= \frac{1}{2}\begin{pmatrix} 0 & |e\rangle\langle e|(\hat{S}_+ + \hat{S}_-)|g\rangle\langle g| \\ |g\rangle\langle g|(\hat{S}_+ + \hat{S}_-)|e\rangle\langle e| & 0 \end{pmatrix} \\
&= \frac{\eta}{2}\hat{\sigma}_x \\
(\hat{S}'_y)^{eg} &= \frac{i}{2}\begin{pmatrix} 0 & |e\rangle\langle e|(\hat{S}_- - \hat{S}_+)|g\rangle\langle g| \\ |g\rangle\langle g|(\hat{S}_- - \hat{S}_+)|e\rangle\langle e| & 0 \end{pmatrix} \\
&= \frac{\eta}{2}\hat{\sigma}_y
\end{aligned} \tag{A2}$$

where η is a measure of the degree of mixing of the spin basis states in the eigenstates of the Hamiltonian. As the absolute energies given by the eigenvalues are meaningless physically, we can re-scale the eigenvalues of $\hat{H}_0$ by adding to it an identity term $-\frac{(\lambda_e+\lambda_g)}{2}\mathbb{1}$ such that λ_e and λ_g are the eigenvalues of eigenvectors $|e\rangle$ and $|g\rangle$ respectively, where $\lambda_e > \lambda_g$. This gives:

$$\hat{H}_0 \mapsto \hat{H}_0^{\varsigma} = \frac{\Omega_0}{2}\hat{\sigma}_z \begin{bmatrix} |e\rangle \\ |g\rangle \end{bmatrix} \oplus \hat{H}_0^{\text{rem}} \tag{A3}$$

such that $\Omega_0 = |\lambda_e - \lambda_g|$. Given a perturbative Hamiltonian of the form in Eq.(24), and assuming that all EPR-allowed transition frequencies are unique, we may solve the Liouville-von Neumann equation for the two-level subsystem in the rotating frame of $\hat{H}_0^{\varsigma}$:

$$\begin{aligned}
\frac{d}{dt}\tilde{\rho}(t) &= i\frac{\omega_1}{2}\left[\tilde{\rho}(t), e^{i\frac{\Omega_0}{2}t\hat{\sigma}_z}\left\{\left(\cos(\Omega_0 t)(\hat{S}'_{x/y})^{eg} + \sin(\Omega_0 t)(\hat{S}'_{y/x})^{eg}\right) + \left(\cos(\Omega_0 t)(\hat{S}'_{x/y})^{eg} - \sin(\Omega_0 t)(\hat{S}'_{y/x})^{eg}\right)\right\} e^{-i\frac{\Omega_0}{2}t\hat{\sigma}_z}\right] \\
&= i\frac{\omega_1\eta}{4}\left[\tilde{\rho}(t), \hat{\sigma}_{x/y}\right] + i\frac{\omega_1\eta}{4}\left[\tilde{\rho}(t), \cos(2\Omega_0 t)\hat{\sigma}_{x/y} - \sin(2\Omega_0 t)\hat{\sigma}_{y/x}\right] \\
&\approx i\frac{\omega_1\eta}{4}\left[\tilde{\rho}(t), \hat{\sigma}_{x/y}\right] \quad \text{if} \quad \omega_1 << \Omega_0.
\end{aligned} \tag{A4}$$

There are two possible regimes for the dynamics of this system. Those for which η is positive, and those for which η is negative. By inspection of the eigenvectors of $\hat{H}_0$ given by Eqs.(8),(9), it becomes clear that the latter occurs only for transitions of type $|-,m\rangle \leftrightarrow |-,m-1\rangle$. Table II shows the form that matrices $(\hat{S}'_{x/y})^{eg}$ take for both regimes; the only one which undergoes a sign change for $\eta < 0$ is the $(\hat{S}'_x)^{eg}$ matrix. This has the effect of inverting the x-axis of the Bloch sphere. In the case that $\eta > 0$, the circular polarisation needed to achieve resonance with the Hamiltonian is of the form $\cos(\Omega_0 t)\hat{S}_{x/y} + \sin(\Omega_0 t)\hat{S}_{y/x}$. We call this the right-handed (RH) field. When $\eta < 0$, the circular polarisation must be of the form $\cos(\Omega_0 t)\hat{S}_{x/y} - \sin(\Omega_0 t)\hat{S}_{y/x}$, which we call the left-handed (LH) field.

	right-handed	left-handed
η	> 0	< 0
$(\hat{S}'_x)^{eg}$	$\frac{1}{2}\begin{pmatrix} 0 & \vert e\rangle\langle e\vert\hat{S}_+\vert g\rangle\langle g\vert \\ \vert g\rangle\langle g\vert\hat{S}_-\vert e\rangle\langle e\vert & 0 \end{pmatrix} = \frac{\vert\eta\vert}{2}\hat{\sigma}_x$	$\frac{1}{2}\begin{pmatrix} 0 & \vert e\rangle\langle e\vert\hat{S}_-\vert g\rangle\langle g\vert \\ \vert g\rangle\langle g\vert\hat{S}_+\vert e\rangle\langle e\vert & 0 \end{pmatrix} = -\frac{\vert\eta\vert}{2}\hat{\sigma}_x$
$(\hat{S}'_y)^{eg}$	$\frac{i}{2}\begin{pmatrix} 0 & -\vert e\rangle\langle e\vert\hat{S}_+\vert g\rangle\langle g\vert \\ \vert g\rangle\langle g\vert\hat{S}_-\vert e\rangle\langle e\vert & 0 \end{pmatrix} = \frac{\vert\eta\vert}{2}\hat{\sigma}_y$	$\frac{i}{2}\begin{pmatrix} 0 & \vert e\rangle\langle e\vert\hat{S}_-\vert g\rangle\langle g\vert \\ -\vert g\rangle\langle g\vert\hat{S}_+\vert e\rangle\langle e\vert & 0 \end{pmatrix} = \frac{\vert\eta\vert}{2}\hat{\sigma}_y$
$(\hat{H}_o^{\varsigma})^{eg}$	$\frac{\Omega_0}{2}\hat{\sigma}_z$	$\frac{\Omega_0}{2}\hat{\sigma}_z$
rotating field	$\cos(\Omega_0 t)\hat{S}_{x/y} +\ sin(\Omega_0 t)\hat{S}_{y/x}$	$\cos(\Omega_0 t)\hat{S}_{x/y} - \sin(\Omega_0 t)\hat{S}_{y/x}$

TABLE II: Pauli operators for the truncated 2-level system under resonance in the right-handed and left-handed regimes. The bottom row indicates the polarisation that the $V_{x/y}(t)$ term must have in order to effect a $e^{-i\frac{\theta}{2}\hat{\sigma}_{x/y}}$ operator in the rotating frame.

Appendix B: Master equation derivation

Taking the Hamiltonian from Eq.(1) and adding to it a perturbative term involving independent temporal magnetic-field fluctuations in all three spatial dimensions, all of which take a Gaussian distribution with mean 0 and variance α_n^2, gives in the interaction picture:

$$\tilde{H}(t) = \sum_{n=1}^{3} \omega_n(t)\tilde{S}_n(t) + \omega_n(t)\delta\tilde{I}_n(t). \tag{B1}$$

We may ignore the nuclear term as its effects will be negligible. We then write the Liouville-von Neumann equation in differential-integral form and take the average over the field fluctuations. Noting that $\langle \frac{d}{dt}\tilde{\rho}(t)\rangle = \frac{d}{dt}\langle\tilde{\rho}(t)\rangle$ we may write this as:

$$\frac{d}{dt}\langle\tilde{\rho}(t)\rangle = i\sum_{n=1}^{3}\langle\omega_n(t)\rangle\left[\langle\tilde{\rho}(t)\rangle, \tilde{S}_n(t)\right] - \sum_{n=1}^{3}\int_{t_0}^{t} ds\langle\omega_n(t)\omega_n(s)\rangle\left[\left[\langle\tilde{\rho}(t)\rangle, \tilde{S}_n^\dagger(t)\right], \tilde{S}_n(s)\right] \tag{B2}$$

where assigning $\tilde{S}_n(t) = \tilde{S}_n^\dagger(t)$ is valid as it is a Hermitian operator. $\langle\tilde{\rho}(t)\rangle$ is the density operator for the nuclear-electronic system, averaged either over an ensemble of such systems, or over many repeated experiments on the same system. Here, we have assumed that the field fluctuation statistics are independent of the quantum state of our system. These assumptions and approximations lead to a Born-Markov master equation. As $\omega_n(t)$ follows a Gaussian distribution with mean 0, the first term of this equation vanishes. Given that the correlation function drops to zero at finite values, we may set the integration limits to $t_0 = 0$ and $t = \infty$, and change the integration constant to $\tau = t - s$. As the temporal fluctuation takes a Gaussian distribution, we may set our correlation functions to be another Gaussian function of the form

$$\langle\omega_n(t)\omega_n(t-\tau)\rangle = \alpha_n^2\frac{1}{2\sqrt{\pi f_n}}e^{-\frac{\tau^2}{4f_n}} \tag{B3}$$

where $f_n = \left(\frac{dB_n}{dt}\right)^{-1}$ is an inverse function of how fast the magnetic field fluctuates. In the limiting case of $\frac{dB_n}{dt} \to \infty$, the correlation function tends to $\alpha_n^2\delta(\tau)$. To aid our calculation, we may write the noise operators in the basis of the eigenstates of $\hat{H}_0$ labeled $|a\rangle$,$|b\rangle$:

$$\begin{aligned} \hat{S}_n &= \sum_{\Omega}\hat{S}_n(\Omega) \\ \hat{S}_n(\Omega) &= \sum_{a,b}\delta(\omega_{ba} - \Omega)|a\rangle\langle a|\hat{S}_n|b\rangle\langle b|. \end{aligned} \tag{B4}$$

Moving such operators to the interaction picture simply gives $e^{-i\Omega t}\hat{S}_n(\Omega)$. This gives:

$$\begin{aligned} \frac{d}{dt}\langle\rho(t)\rangle &= -\alpha_n^2\sum_{n=1}^{3}\sum_{\Omega,\Omega'}\int_0^\infty d\tau\frac{1}{2\sqrt{\pi f_n}}e^{-\frac{\tau^2}{4f_n}}e^{i\Omega\tau}e^{it(\Omega'-\Omega)} \times \\ &\left[\left[\langle\tilde{\rho}(t)\rangle, \hat{S}_n^\dagger(\Omega')\right], \hat{S}_n(\Omega)\right]. \end{aligned} \tag{B5}$$

If $\alpha^2 << \Omega, \Omega'$, meaning that the dynamic time scale of our system is much shorter than that of the decoherence caused by the magnetic-field fluctuation, which is a reasonable assumption for systems of interest, we may make the rotating wave approximation (often also referred to as the secular approximation) and drop all terms where $\Omega \neq \Omega'$. Furthermore, noting that $[A,[B,C]] = ABC - BCA + H.C.$ (Hermitian conjugate) if A, B, C are Hermitian operators leads to :

$$\begin{aligned} \frac{d}{dt}\langle\rho(t)\rangle &= \alpha_n^2\sum_{i=n}^{3}\sum_{\Omega}\int_0^\infty d\tau\frac{1}{2\sqrt{\pi f_n}}e^{-\frac{\tau^2}{4f_n}}e^{i\Omega\tau} \times \\ &\left(\hat{S}_n^\dagger(\Omega)\langle\tilde{\rho}(t)\rangle\hat{S}_n(\Omega) - \langle\tilde{\rho}(t)\rangle\hat{S}_n^\dagger(\Omega)\hat{S}_n(\Omega)\right) \\ &+H.C. \end{aligned} \tag{B6}$$

We may decompose the integrand to

$$\int_0^{\infty} d\tau \frac{1}{2\sqrt{\pi f_n}} e^{-\frac{\tau^2}{4f_n}} e^{i\Omega\tau} = \gamma_n(\Omega) + i\Gamma_n(\Omega) \tag{B7}$$

where:

$$\begin{aligned} \gamma_n(\Omega) &= \frac{1}{2}\int_{-\infty}^{\infty} d\tau \frac{1}{2\sqrt{\pi f_n}} e^{-\frac{\tau^2}{4f_n}} e^{i\Omega\tau} = \frac{1}{2} e^{-f_n\Omega^2} \\ \Gamma_n(\Omega) &= \frac{1}{2i}\int_0^{\infty} d\tau \frac{1}{2\sqrt{\pi f_n}} e^{-\frac{\tau^2}{4f_n}} \left(e^{i\Omega\tau} - e^{-i\Omega\tau}\right). \end{aligned} \tag{B8}$$

Plugging these expressions into Eq.(B6), and moving back into the Schrodinger picture, gives us our final master equation:

$$\frac{d}{dt}\langle\rho(t)\rangle = i\left[\langle\rho(t)\rangle, \hat{H}_0 + \hat{H}_{LS}\right] + \alpha_n^2 \sum_{n=1}^{3}\sum_{\Omega} e^{-f_n\Omega^2} \times \left(\hat{S}_n^{\dagger}(\Omega)\langle\tilde{\rho}(t)\rangle\hat{S}_n(\Omega) - \frac{1}{2}\left[\langle\tilde{\rho}(t)\rangle, \hat{S}_n^{\dagger}(\Omega)\hat{S}_n(\Omega)\right]_+\right) \tag{B9}$$

where

$$H_{LS} = \sum_n \sum_{\Omega} \Gamma_n(\Omega)\hat{S}_n^{\dagger}(\Omega)\hat{S}_n(\Omega) \tag{B10}$$

is the Lamb shift and changes the energy levels of the system. This is a negligible effect and hence can be ignored. We use $[A, B]_+ := AB + BA$ as the anticomutator operator.

[1] B. E. Kane, Nature, **393**, 133 (1998).

[2] S. R. Schofield, N. J. Curson, M. Y. Simmons, *et al.* Phys. Rev. Lett. **91**, 136104 (2003); A. M. Tyryshkin, S. A. Lyon, A. V. Astashkin, A. M. Raitsimring, Phys. Rev. B **68**, 193207 (2003); Kai-Mei C. Fu, T. D. Ladd, Santori C. *et al.* Phys. Rev. B **69**, 125306 (2004); G. W. Morley, D. R. McCamey, H. A. Seipel *et al.*, Phys. Rev. Lett **101**, 207602 (2008); J. J. L.Morton, A. M. Tyryshkin, R. M. Brown, *et al.* Nature, **455**, 1085 (2008); A. Morello *et al.* Nature **467**, 687-691 (2010); D. R. McCamey, C. Boehme, G. W. Morley, J. van Tol, arxiv:1109.1326 (2011); P. T. Greenland, S. A. Lynch, A. F. G. van der Meer, B. N. Murdin, C. R. Pidgeon, B. Redlich, N. Q. Vinh and G. Aeppli, Nature **465**, 1057 (2010); M. Steger, T. Sekiguchi, A. Yang, K. Saeedi, M. E. Hayden, M. L. W. Thewalt, K. M. Itoh, H. Riemann, N. V. Abrosimov, P. Becker, and H. J. Pohl, Journal of Applied Physics **109**, 102411 (2011); S. Simmons, R. M. Brown, H. Riemann, N. V. Abrosimov, P. Becker, H. J. Pohl, M. L. W. Thewalt, K. M. Itoh, and J. J. L. Morton, Nature **470**, 69 (2011).

[3] H. Morishita, L. S. Vlasenko, H. Tanaka *et al.*, Phys. Rev. B **80**, 205206 (2009).

[4] G. W. Morley, M. Warner, A. M. Stoneham *et al.*, Nature Materials **9**, 725-729 (2010)

[5] R. E. George, W. Witzel, H. Riemann *et al*, Phys. Rev. Lett. **105**, 067601.

[6] T. Sekiguchi, M. Steger, K. Saeedi, M. Thewalt *et al.*, Phys. Rev. Lett **104** 137402 (2010)

[7] M. H. Mohammady, G. W. Morley and T. S. Monteiro, Phys. Rev. Lett. **105**, 067602 (2010)

[8] M. Belli, M. Fanciulli and N. V. Abrosimov, Phys. Rev. B **83**, 235204 (2011)

[9] W. M. Witzel and S. Das Sarma, Phys. Rev. B **74**, 035322 (2006)

[10] Wen Yang and Ren-Bao Liu, Phys. Rev. B **78**, 085315 (2008)

[11] Alexei M. Tyryshkin et al, arxiv:1105.3772 (2011)

[12] A. Schweiger and G. Jeschke,“*Principles of Pulse paramagnetic resonance*” Oxford (2001).

[13] G. W. Morley, P. Lueders, M. H. Mohammady, G. Aeppli, C. W. M. Kay, G. Jeschke and T. S. Monteiro, arXiv:1109.4269 (2011)

[14] G. Ithier *et al.*, Phys. Rev. B **72**, 134519 (2005); D. Vion *et al.* Science **296**, 886 (2002).

[15] At $\omega_0 = 5A$, there is a small difference between $f(10 \to 9)$ and $f(11 \to 10)$. Including the nuclear terms, the frequencies equalize at field shifted by $\sim 10^{-3}$ from $\omega_0 = 5A \approx 0.26$T.

[16] G Mitikas, Y Sanakis and G Papavassiliou, Phys.Rev.A **81**, 020305 R (2010).

[17] D. P. Divincenzo, Phys. Rev. A **51**, 1015 (1995).

[18] Michael A. Nielsen and Issac L. Chuang, *“Quantum Computation and Quantum Information”*, Cambridge university press, (2000)

[19] G. Burkard, D. Loss, D. P. Di Vincenzo, J. A. Smolin,Phys. Rev. B **60**, 11404 (1999)

[20] P. W. Anderson, “*Concepts in Solids*”, Addison Wesley, Redwood City (1963).

[21] N. Schuch, J. Siewert, Phys. Rev. A **67**, 032301 (2003)

[22] Y. Makhlin, Quant. Info. Proc. 1, 243-252 (2002)

[23] G. Feher, E. A. Gere, Phys. Rev. **114**(5), 1245 (1959)

[24] T. G. Castner, Phys. Rev. **155**(3), 816 (1967)

[25] H. P. Breuer and F. Petruccione, “*The Theory of Open Quantum Systems*”, Oxford University Press, (2007)

[26] D. M. Tong, K. Singh, L. C. Kwek and C. H. Oh, Phys. Rev. Lett. **95**, 110407 (2005)

[27] D. P. S. McCutcheon, A. Nazir, S. Bose and A. J. Fisher, Phys. Rev. A **80**, 022337 (2009)